TẠP CHÍ KHOA HỌC VÀ CÔNG NGHỆ ĐẠI HỌC DUY TÂN
DTU Journal of Science and Technology 05(78) (226) 43-53
ĐẠI HỌC DUY TÂN
DUYTAN UNIVERSITY

Green Synthesis of Ce-doped ZnO Nanoparticles Using *Hedyotis capitellata* Leaf Extract for Photocatalytic Degradation of Methyl Orange

Tổng hợp xanh vật liệu nano ZnO pha tạp Ce sử dụng dịch chiết lá *Hedyotis capitellata* và ứng dụng quang xúc tác phân hủy Methyl Orange

Vien Thi Thuy[a], Nguyen Thi Ngoc Anh[b], Doan Van Dat[c*], Phung Thi Cam Loan[d]
Viên Thị Thủy[a], Nguyễn Thị Ngọc Anh[b], Đoàn Văn Đạt[c*], Phùng Thị Cẩm Loan[d]

[a]*Office of Academic Affairs, Industrial University of Ho Chi Minh City, No. 12 Nguyen Van Bao Street, Hanh Thong Ward, Ho Chi Minh City, 71423, Vietnam*
[a]*Phòng Đào tạo, Trường Đại học Công nghiệp Thành phố Hồ Chí Minh, Số 12 đường Nguyễn Văn Bảo, phường Hạnh Thông, thành phố Hồ Chí Minh, 71423, Việt Nam*
[b]*Nguyen Duc Mau High School, Thanh Son Hamlet, Quynh Phu Commune, Nghe An Province, 43541, Vietnam*
[b]*Trường Trung học Phổ thông Nguyễn Đức Mậu, thôn Thanh Sơn, xã Quỳnh Phú, tỉnh Nghệ An, 43541, Việt Nam*
[c]*Faculty of Chemical Engineering, Industrial University of Ho Chi Minh City, No. 12 Nguyen Van Bao Street, Hanh Thong Ward, Ho Chi Minh City, 71423, Vietnam*
[c]*Khoa Công nghệ Hóa học, Trường Đại học Công nghiệp Thành phố Hồ Chí Minh, Số 12 Nguyễn Văn Bảo, phường Hạnh Thông, thành phố Hồ Chí Minh, 71423, Việt Nam*
[d]*Faculty of Natural Sciences Education, Dong Nai University, No. 9 Le Quy Don Street, Tam Hiep Ward, Dong Nai City, 76109, Vietnam*
[d]*Khoa Sư phạm Khoa học Tự nhiên, Trường Đại học Đồng Nai, Số 9 đường Lê Quý Đôn, phường Tam Hiệp, thành phố Đồng Nai, 76109, Việt Nam*

(Date of receiving article: 16/09/2026, date of completion of review: 28/09/2026, date of acceptance for posting: 16/10/2026)

Abstract

This work presents a green route to synthesize single phase Ce-doped ZnO nanoparticles using the aqueous leaf extract of *Hedyotis capitellata* (HC-Ce@ZnO) as an effective reactant. The phase composition and crystalline nature of HC-Ce@ZnO with different weight% Ce doping were confirmed by powder X-ray diffraction (XRD). The organic functional groups possibly responsible for the transformation of Zn^{2+} into ZnO nanoparticles were recognized by Fourier transform infrared spectroscopy (FTIR). The transmission electron microscope (TEM) image revealed that HC-Ce@ZnO nanoparticles were mostly in spherical shape with sizes ranging from 2-6 nm. The biosynthesized Ce-doped ZnO nanoparticles were then evaluated for their photocatalytic activity toward the degradation of methyl orange (MO) using UV-Vis spectroscopy. The results showed that Ce^{3+} ions were successfully integrated into ZnO structure to form single crystals of Ce@ZnO with the particle size in the range of 2-6 nm. The optimal 1%Ce-doped ZnO nanoparticles can remove 92% MO within 240 min under visible light irradiation. The photocatalytic degradation kinetics followed a pseudo-first-order model, with an apparent rate constant of $k = 0.0133$ min^{-1}.

Keywords: Green synthesis, Ce-doped ZnO, nanoparticles, methyl orange, photocatalytic degradation

[*]*Corresponding author:* Doan Van Dat
Email: doanvandat@iuh.edu.vn

Tóm tắt

Nghiên cứu này trình bày phương pháp tổng hợp xanh các hạt nano ZnO pha tạp Ce đơn pha (HC-Ce@ZnO), sử dụng dịch chiết lá *Hedyotis capitellata* trong nước làm tác chất. Thành phần pha và cấu trúc tinh thể của HC-Ce@ZnO với các hàm lượng Ce pha tạp khác nhau theo phần trăm khối lượng được xác định bằng phương pháp nhiễu xạ tia X (XRD). Các nhóm chức hữu cơ có thể tham gia vào quá trình chuyển hóa Zn^{2+} thành các hạt nano ZnO được nhận diện bằng phổ hồng ngoại biến đổi Fourier (FTIR). Ảnh hiển vi điện tử truyền qua (TEM) cho thấy các hạt nano HC-Ce@ZnO chủ yếu có dạng hình cầu, với kích thước từ 2-6 nm. Hoạt tính quang xúc tác của các hạt nano ZnO pha tạp Ce được đánh giá thông qua quá trình phân hủy methyl orange (MO), sử dụng phương pháp quang phổ UV-Vis. Kết quả cho thấy các ion Ce^{3+} đã được tích hợp thành công vào cấu trúc ZnO, tạo thành các đơn tinh thể Ce@ZnO có kích thước từ 2-6 nm. Mẫu ZnO pha tạp 1% Ce cho hiệu quả tối ưu, loại bỏ 92% MO trong 240 phút dưới điều kiện chiếu sáng khả kiến. Động học phân hủy xúc tác quang tuân theo mô hình bậc nhất biểu kiến, với hằng số tốc độ k = 0,0133 $phút^{-1}$.

Từ khóa: Tổng hợp xanh, ZnO pha tạp Ce, hạt nano methyl orange, quang xúc tác

1. Introduction

Metal oxides and their based nanomaterials have attracted considerable attention in the last decade because of their exceptional properties and potential applications in every areas of science and technology [1]. ZnO nanoparticles (NPs) are considered as a multifunctional material because of their unique physical and chemical properties that are successfully applied in many fields of the industries like pharmaceutical, cosmetic, textile, rubber processing, electronic, and photo-catalysis [2]. The main and frequently used synthetic methods of ZnO NPs are probably chemical, hydrothermal and sol-gel processes taking place in the liquid phase due to a self-aggregation, in which ordered aggregates are formed by spontaneous chemical process in the presence of necessary precursors and may be pH regulators [3, 4]. However, it is still a big challenge to develop a simple and eco-friendly method for possible industrial scale production of ZnO NPs with designed chemical components by doping inorganic transition metal ions, which strongly affect the properties of the host nanomaterial [5]. Recently, the green synthesis of ZnO NPs based on plant extracts has received much interest due to its simplicity, low cost and environmental friendliness [6]. The method involves the use of extract from various parts of plant such as leaves, fruits, peels, stems, roots, and seeds as appropriate reactants and stabilizing agents to control the formation of ZnO NPs with desired particle size range [7]. Many studies have reported that the bioactive organic compounds present in the extracts, especially polyphenols act as effective reactants and biomolecules containing amino and carboxylic groups play role as stabilizers, promoting the conversion of nano-sized ZnO [8].

Hedyotis capitellata (HC), a species belonging to the Rubiaceae family, is an erect or decumbent plant that grows well in dry, sandy soils along rivers and coasts and in forests [9]. It is found in abundance in the rainforests of Southeast Asia, and usually used as an effective traditional medicine for treating inflammations of stomach, tongue and throat. The plant also serves as a poultice for snakebites, broken bones, bruises and rheumatism [10]. The phytochemistry of HC is mainly characterized by the occurrence of iridoids, indole alkaloids, β-carboline alkaloid, capitelline, and flavonoids [11]. It was proved that, the hydroxyl groups in multifunctional alcohol compounds present in plant extracts are responsible for the formation of ZnO from Zn^{2+} [12]. Chelate complexes form between Zn^{2+} ions and hydroxyl groups at temperatures below 100 °C. Upon heating to higher temperatures, these complexes decompose to form ZnO. Other organic compounds in the extract also act as a protective layer, keeping the newly formed nanoparticles from agglomeration [13].

Zinc oxide has been proved to be a dynamic photocatalyst in the UV region thanks to its appropriate band gap energy of 3.2 eV (λ = 387 nm) [14]. However, ZnO shows quite poor photocatalytic properties in the visible region, including sunlight because the solar spectrum consists of only 5–7% of UV light [15]. To enhance photocatalytic performance, many elements, such as Ag, Nb, Fe, Cu, Mn, Al, etc...were integrated into the structure of ZnO to lower its band gap [16-19]. Among them, cerium (Ce) presents itself as a potential candidate. The rare earth ions of Ce^{3+} have numerous energy levels, plenty of metastable states, and a good ability of integration into ZnO wurtzite structure without appearance of impurities [20, 21]. Doping ZnO with Ce^{3+} ions can enhance its photocatalytic activity by narrowing the band gap energy, thereby utilizing the visible region of sunlight [22].

Over the past few decades, with the rapid development of many industries, especially dye-stuffs and the textile industry, water pollution has become a serious environmental problem. The release of excess dyes into water sources strongly affects both human life and the biosphere. Among them, MO is the most useful synthetic dye with high toxic nature used in various industries like papers, textiles industry, plastics, and cosmetics industries. The discharge of MO into the water environment can cause skin diseases, vomiting and diarrhea [23]. The removal of MO from wastewater by photocatalytic degradation using semiconductors such as ZnO NPs in the existence of UV/Visible light is one of the most common techniques owing to its many advantages [24, 25]. Hence, in this present work, we describe a simple green synthesis of single crystal phase of ZnO NPs with different Ce-doping levels by HC leaves extract without using any expensive toxic commercial reductant and stabilizer for the first time. The photocatalytic performance of HC-Ce@ZnO toward MO under visible light irradiation as well as the mechanism of MO degradation were also investigated.

2. Materials and methods

2.1. Materials

Zinc nitrate hexahydrate ($Zn(NO_3)_2.6H_2O$, 99.99%) and cerium(III) nitrate hexahydrate ($Ce(NO_3)3.6H_2O$, 99.99%) were analytical grade reagents supplied by Himedia Chemical Company (India). Methyl orange ($C_{14}H_{14}N_3NaO_3S$, ≥99.8%) of reagent grade was purchased from Merck (Germany). Isopropanol (C_3H_8O, 99%, IP), sodium hydroxide (NaOH, 98.5%), hydrochloric acid (HCl, 36.5%), and disodium ethylenediaminetetraacetate dihydrate ($C_{10}H_{14}N_2Na_2O_8.2H_2O$, Na_2EDTA) were supplied by Xilong Chemical Co., Ltd. (Shantou, China). Dried HC leaves with the humidity about 10% were purchased in an herbal store in Ho Chi Minh city (Vietnam).

2.2. Preparation of HC extract

The powder of dried HC (10 g) was put into distilled water (200 mL) and kept heating at 90ºC with reflux for 1 hour. The mixture was cooled down after that to room temperature. The aqueous HC leaves extract was obtained by filtering the mixture with Whatman No.1 filter paper. The freshly prepared extract was used for all experiments.

2.3. Fabrication of HC-Ce@ZnO

The synthesis procedure of Ce-doped ZnO nanoparticles was illustrated in Figure 1. A similar procedure for the biosynthesis of undoped ZnO NPs was described in [26]. Briefly, 2.000 g of $Zn(NO_3)_2 \cdot 6H_2O$ and 0.0174, 0.0526, or 0.0890 g of $Ce(NO_3)_3 \cdot 6H_2O$ were dissolved in 100 mL of freshly prepared HC leaf extract. The mixture was stirred for 1 h and then heated in a thermostatic bath at 70°C for approximately 3 h, until a viscous precursor was formed. The precursor was calcined at 400 °C

for 1 h. After cooling, the product was ground into a fine powder and stored in a desiccator. Undoped ZnO was prepared under identical conditions without the Ce precursor.

The nominal Ce content was defined as $100.m_{Ce}/(m_{Ce} + m_{ZnO})$, where m_{Ce} is the mass of elemental Ce introduced and $m_{ZnO}$is the theoretical mass of ZnO calculated from the Zn precursor. The Ce precursor masses of 0.0174, 0.0526, and 0.0890 g correspond to nominal Ce contents of approximately 1%, 3%, and 5%, respectively. The resulting samples were designated HC-1%Ce@ZnO, HC-3%Ce@ZnO, and HC-5%Ce@ZnO; the undoped sample was designated HC-ZnO.

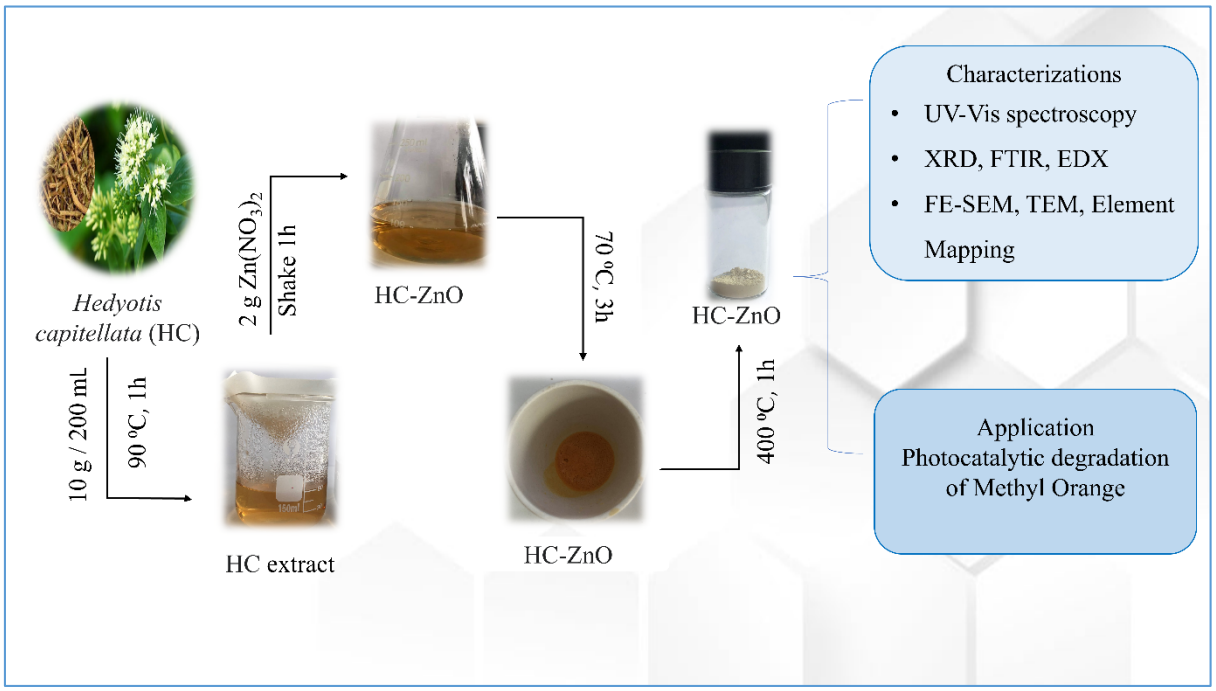


Figure 1. Schematic illustration for biosynthesis of HC-Ce@ZnO nanoparticles and its application

2.4. Characterization methods

Powder X-ray diffraction patterns were recorded in a Shimadzu 6100 X-ray diffractometer (Japan) with a Cu K excitation source at a scan rate of 1.0º/min in the two-theta range of 5–80º. The surface morphology of the synthesized catalysts was examined on a field emission scanning electron microscope Hitachi S-4800 HI-9057-0006 (Japan) and a transmission electron microscope FEI Tecnai G2-20 (Japan) operated at 15 kV and 100 kV accelerating voltage, respectively. The elemental analysis was conducted using energy-dispersive X-ray spectroscopy, attached to the SEM. Fourier transform infrared spectra were recorded on an EQUINOX 55 spectrometer (Bruker, Billerica, MA, USA). The optical absorption characteristics of the photocatalysts were determined by UV-Vis diffuse reflectance spectroscopy (Shimadzu UV-2450, Kyoto, Japan) in the range of 300-900 nm. The Brunauer-Emmett-Teller surface areas were measured using a Quantachrome NOVA 4000e (Florida, USA).

2.5. Photocatalytic degradation

The photocatalytic activities of the ZnO and Ce-doped ZnO samples toward the degradation of anionic MO were examined under visible light at 25 ºC maintained by a water-cooling jacket [27]. Photocatalytic reactions were carried out under the light irradiation supplied from an Osram mercury vapor lamp 250W (USA) as simulated sunlight. The pH of MO solutions was adjusted by 0.1 M HCl or 0.1 M

NaOH. Before illumination, a mixture consisting of MO aqueous solution (10 ppm, 100 mL) and the given catalyst (50 mg) was magnetically stirred in the dark for 60 min to reach the adsorption-desorption equilibrium of the dye on the catalyst surface. Then, 5 mL of the suspension was taken out after a regular time interval and centrifuged to remove the photocatalyst. The MO concentration in the remaining solution was monitored by measuring the absorption intensity at its maximum absorbance wavelength of λ = 464 nm using a UV-visible Metash spectrophotometer (Model 5100, China) in a 1 cm path length spectrometric quartz cell.

2.6. *Active species trapping experiments*

The active species generated during the early stages of photocatalytic processes responsible for MO degradation were determined by an indirect chemical probe method. The trapping tests for the photocatalytic degradation of MO involved incorporation of different reagents in the systems. They have high affinities for different oxidizing radicals as isopropanol for hydroxyl species, Na_2EDTA for electron-hole pairs. The trapping experiments were conducted similarly to the mentioned above photocatalytic experiments, except that the chemical agents (5 mM isopropanol and 5 mM Na_2EDTA) are added before the beginning of the photocatalytic experiment.

3. Results and discussion

3.1. Characterization of ZnO and Ce-doped ZnO

3.1.1. Structure and surface properties

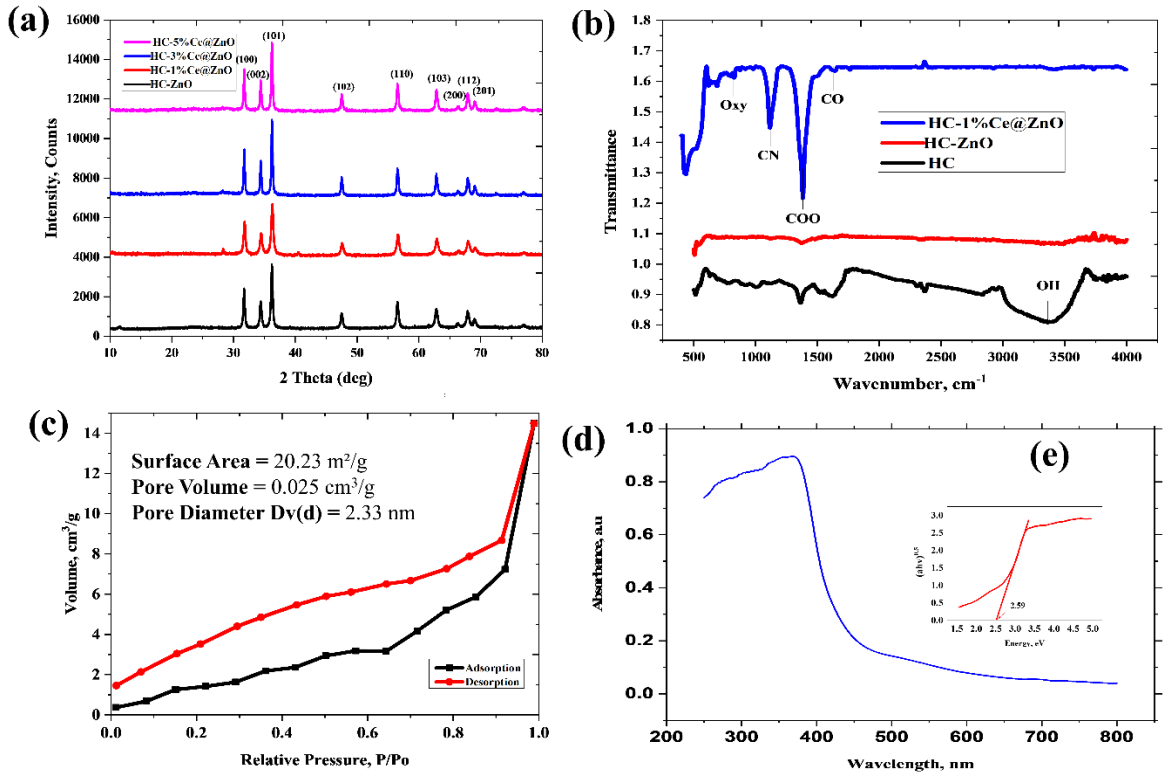


Figure 2. XRD patterns of ZnO with different Ce-doping levels (a), FTIR spectra of HC extract, ZnO and 1%Ce@ZnO (b), N_2 adsorption-desorption isotherm of 1%Ce@ZnO (c), DRS spectrum of 1%Ce@ZnO (d) and insert of plot $(ahv)^{0.5}$ – hv (e)

The as-prepared HC-ZnO and HC-Ce@ZnO samples were characterized by XRD to determine their crystal structural features and grain sizes. Figure 2a shows the XRD patterns of

undoped ZnO and different weight% Ce-doped ZnO samples. The diffraction peaks appeared at 2θ = 32.2°, 34.9°, 36.78°, 47.94°, 57.08°, 63.32°, and 68.34° corresponding to (100), (002), (101), (102), (110), (103), and (112) planes, respectively indicated the wurtzite single crystalline phase of pure ZnO [26]. No crystalline impurities were observed, even at the high content of Ce. However, a slight shift of diffraction peaks for Ce-doped ZnO toward higher diffraction angles was observed as the doping percentage increased from 1 to 5% due to the substitution of Ce in the ZnO crystal. The average crystalline size of the biosynthesized HC-ZnO and 1%, 3% and 5% Ce -doped ZnO evaluated using the Debye-Scherrer formula were found to be 28, 21, 35 and 38 nm, respectively. It can be seen that the crystalline size tends to decrease with a small amount of Ce integrated, but increases gradually as the amount of Ce increases. The HC-1%Ce@ZnO sample has the most optimal crystalline size, smaller than that of HC-ZnO. The decrease in the crystallite size of HC-1%Ce@ZnO sample compared to pure ZnO sample can be explained by the restricted growth of crystal grains due to formation of Ce-O-Zn linkages in the doped samples. Thus, the HC-1%Ce@ZnO sample is likely to be the most promising material for MO degradation.

The FTIR spectra of undoped HC-ZnO, HC-1%Ce@ZnO, and the HC dried extract are presented in Figure 2b. The absorption peaks characterized for covalent bonds in the functional groups of organic compounds present in the HC extract were observed at 1049, 1109, 1384, 1446, 1633, 2854, 2923 and 3420 cm^{-1}. As can be seen in the FTIR spectrum of HC extract, the characteristic broad band of OH groups with the peak centered at 3420 cm^{-1} proves the existence of multi-functional alcohol compounds. However, those OH groups completely disappeared on the FTIR spectra of ZnO and Ce-doped ZnO. It can be concluded that the alcohol compounds present in the extract played a key role in the formation of ZnO and Ce-ZnO nanomaterials. The OH^- groups could create complex bonds with Zn^{2+} ions in the solution at room temperature. These bonds were destroyed in the calcined stage at high temperature, forming ZnO [12, 27]. Besides, the FTIR spectrum of HC extract also shows the absorption peaks at 1633 cm^{-1} and 1049 cm^{-1}, assigned to stretching vibrations of C=O and C-O functional groups, respectively. The peaks at about 1400 and 1030 cm^{-1} are related to vibrations of N-H and C-N bonds in proteins. Due to the calcination process, the number of organic functional groups in ZnO and Ce-ZnO samples is significantly reduced, compared to those of the HC extract sample. Almost no organic molecules appeared in the ZnO sample; meanwhile the Ce-doped ZnO still retains the organic functional groups as the HC extract, except for OH groups. This can be explained by the difference in ion charge between Ce^{3+} and Zn^{2+}. The Ce-doped ZnO with Ce^{3+} on its surface can attract more organic molecules through the functional groups than ZnO. The organic compounds in the extract also act as a protective layer, enclosing the newly formed nanoparticles, helping the particles avoid agglomeration, and keeping the particles in nano size.

The textural properties of HC-1%Ce@ZnO were evaluated by N_2 adsorption-desorption analysis (Figure 2c). The isotherm exhibited a hysteresis loop over a relative pressure range of approximately 0.4-0.95, consistent with capillary condensation. The specific surface area and total pore volume were 20.23 m^2/g and 0.025 cm^3/g, respectively. The average pore diameter was 2.33 nm, close to the lower limit of the mesopore range.

The UV–Vis DRS used to examine the optical properties of the biosynthesized HC-1%Ce@ZnO sample were presented in Figure 2d. The Tauc plot of $(\alpha h\nu)^{0.5}$ versus $h\nu$ derived from UV–Vis DRS result for 1% Ce-doped ZnO sample is also built and shown as inset in Fig 2(e). The band gap energy (Eg) can be calculated by using the Kubelka–Munk formula $(\alpha h\nu)^{0.5} = A(h\nu - E_g)$; where α, h, ν, E_g, and A correspond to the absorption coefficient, Planck's constant, light frequency, the band gap energy, and the constant, respectively. The absorbance spectra demonstrated that the 1%Ce-doped ZnO sample possess a broad absorption tail band in the visible region between 400 and 600 nm. The E_g value estimated for HC-1%Ce@ZnO sample from the linear extrapolation of $(\alpha h\nu)^{0.5}$ versus (hν) is 2.59 eV, which is much lower compared with Ce-doped ZnO synthesized by different methods. The reduction in the energy band gap of HC-1%Ce@ZnO biosynthesized by the HC extract may be due to the following reason. Besides the well-known effect of Ce dopant carbon derived from organic substances calcined at high temperature also plays an important role in reducing the band gap of ZnO by improving the separation efficiency of photogenerated electron−hole pairs, thereby enhancing the photocatalytic activity of ZnO.

3.1.2. Morphological and compositional studies

The SEM images of HC-ZnO and HC-1%Ce-ZnO, and TEM micrographs of HC-1%Ce@ZnO are shown in Figures 3a, 3b and 3c, respectively. As seen in Figure 3a and 3b, the HC-ZnO and HC-1%Ce@ZnO samples have a quite similar surface morphology. Both samples exhibited facets characteristic of the hexagonal wurtzite structure, which assembled into larger crystals. Figure 3c depicts the TEM imagery of the biosynthesized HC-1%Ce@ZnO nanoparticles, where the morphological topography illustrates nanospheres with diameter in the range 2-6 nm. Moreover, the EDX spectrum shown in Figure 3(d) confirmed the presence of Zn, O and Ce elements with the weight percentages of 74.8% and 22.73%, 2.47% and atomic percentages of 44.3%, 55.01%, and 0.68% (Insert in Figure 3d), respectively.

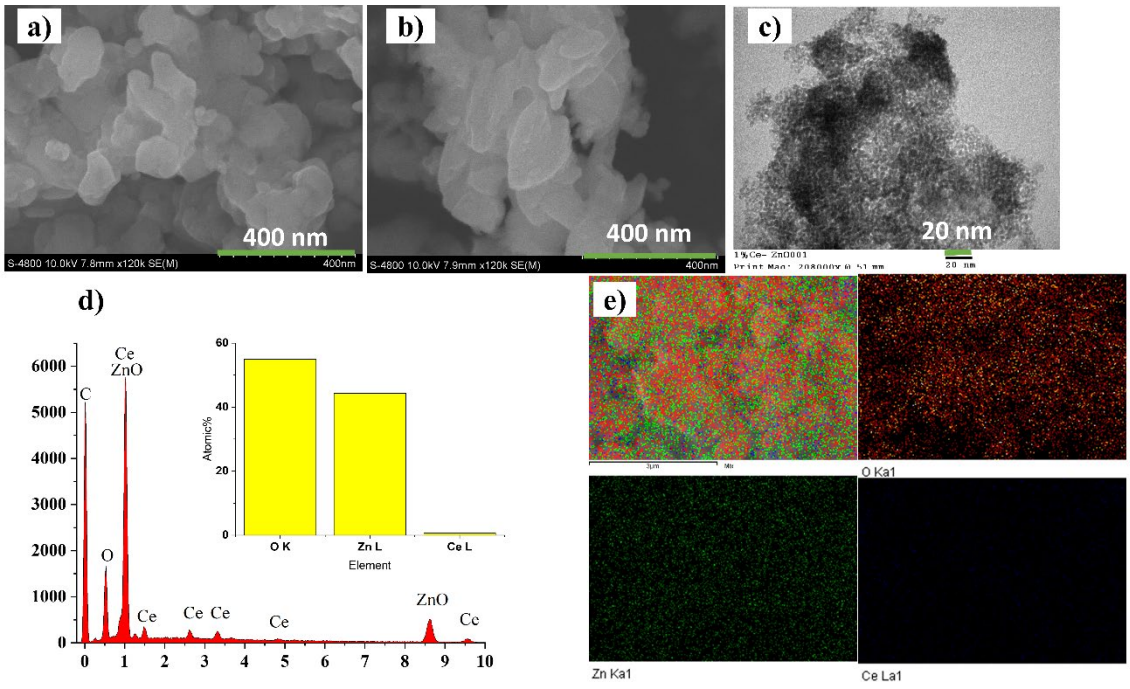


Figure 3. SEM images of ZnO (a), SEM images of 1%Ce@ZnO sample (b), TEM image of 1%Ce@ZnO sample (c), EDX spectrum (d) and Element mapping of 1%Ce@ZnO sample (e)

In addition, the carbon signal in the EDX spectrum may indicate the presence of residual organic compounds from the HC extract on the surface of the ZnO nanoparticles. The distribution of the elements in the material was investigated by element mapping technology as depicted in Figure 3e. The element mapping showed their uniform distribution on the surface. This even distribution will improve the contact between organic molecules of pollutants and active sites on the surface of the material, thereby enhancing its photocatalytic capability.

3.1.3. Photocatalytic activities

Photocatalytic activity for degradation of MO obeys the pseudo-first-order reaction kinetics with k as the rate constant and t as the UV irradiation time given by the equations as follows:

$$\ln(C_0/C_t) = kt \quad (1)$$

where C_0 is the MO concentration at the start of irradiation, after dark adsorption - desorption equilibrium; C_t is the MO concentration after an irradiation time t; and k is the apparent pseudo-first-order rate constant (min^{-1}).

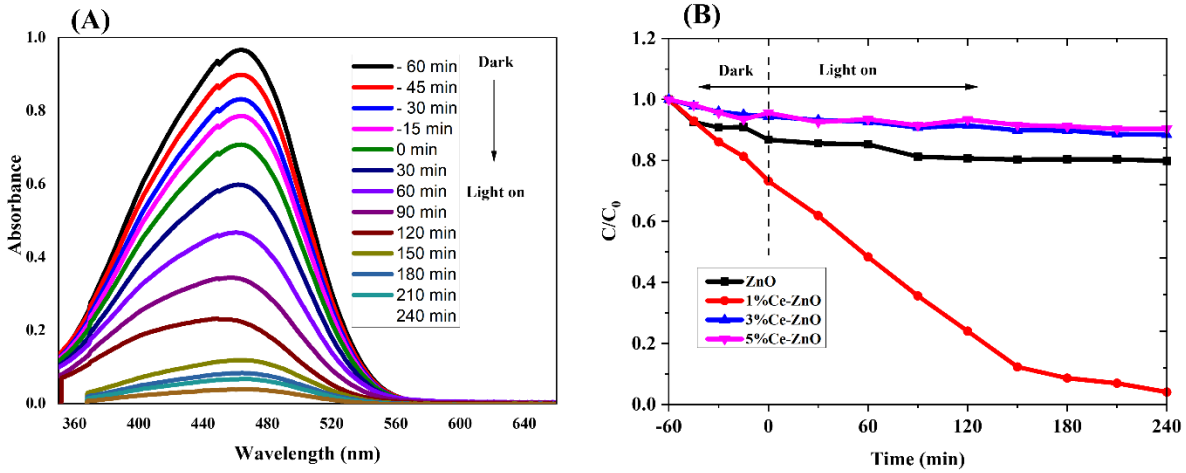


Figure 4. (a) UV–Vis absorption spectra of MO in the presence of HC-1%Ce@ZnO; (b) C/C_0 changes with irradiation time for HC-ZnO, HC-1%Ce@ZnO, HC-3%Ce@ZnO, and HC-5%Ce@ZnO.

Figure 4a shows the time-dependent UV-Vis absorption spectra of MO in the presence of HC-1%Ce@ZnO. The absorbance at the characteristic wavelength of 464 nm decreased progressively during irradiation, indicating MO decolorization. Figure 4b compares the changes in normalized MO concentration (C/C_0) for HC-ZnO and the three Ce-doped samples. Among the four materials tested, HC-1%Ce@ZnO showed the greatest decrease in C/C_0 over 240 min. A linear fit of $\ln\left(\frac{C_0}{C}\right)$ against irradiation time for HC-1%Ce@ZnO yielded an apparent pseudo-first-order rate constant of 0.0133 min^{-1}, with $R^2 = 0.99$.

Scavenging experiments of the active species (•OH and electron-hole pairs) were conducted to confirm the nature of photocatalytic degradation. Isopropanol and Na_2EDTA have been proved as effective scavengers for •OH radicals and electron-hole pairs. In the presence of them, the amount of •OH radicals and electron-hole pairs will be reduced, consequently, the rate of photocatalytic degradation of MO was slowed down. Indeed, the scavenging experiment results revealed a reduction in the degradation efficiency toward 10 mg/L MO solution to 47.5% and 43.7% by the impact of IP and Na_2EDTA, respectively (Figure 5a). It suggested that the photogenerated electronhole pairs and hydroxyl radicals are the main oxidizing agents in the degradation process using the biosynthesized Ce-doped ZnO NPs. Due to doping Ce and the presence of small amount of C in ZnO structure, a new electronic

state (intermediate energy state) appears right inside the bandgap of ZnO by the interaction of Ce's 4f orbitals and 2p orbital of C with the valence or conduction region of ZnO. The distance of charge transfer between the 4f electrons of the dopant cerium ions or 2p electrons of the carbon ions and the conduction band (CB) or the valence band (VB) of ZnO is shortened, thus enhancing the light absorption of the composite in visible region [27].

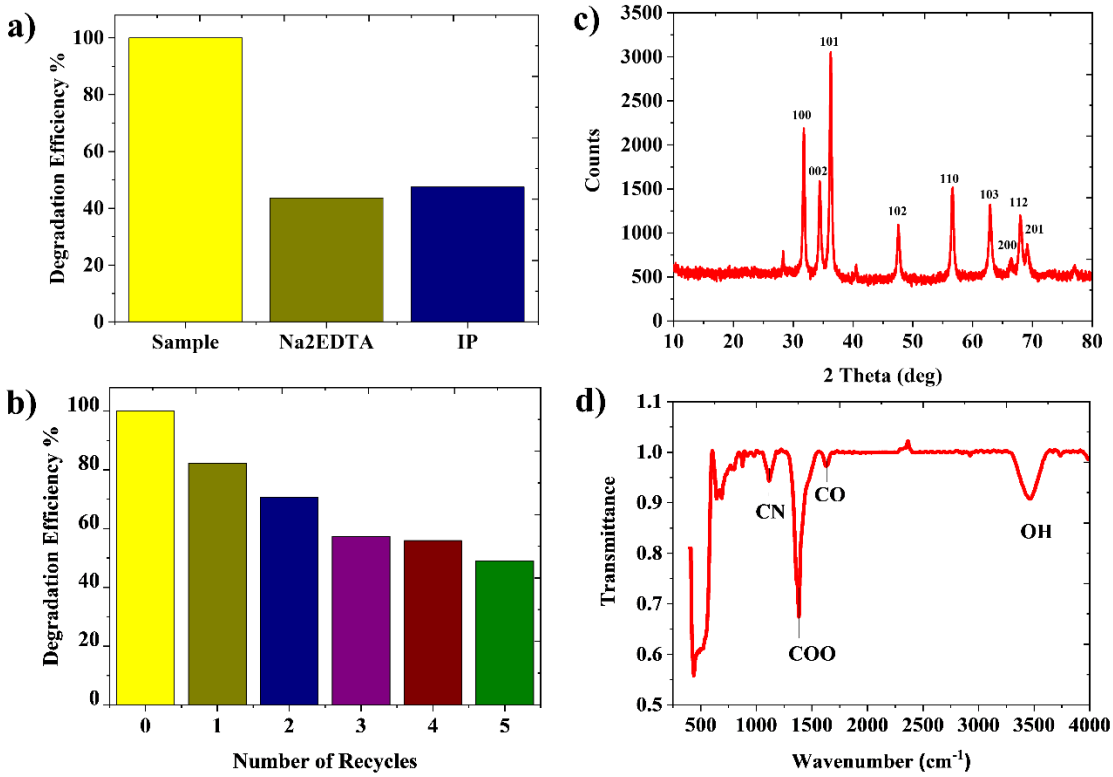


Figure 5. (a) Effect of Na_2EDTA and isopropanol on MO degradation in the presence of HC-1%Ce@ZnO; (b) degradation efficiency over five reuse cycles; (c) XRD pattern and (d) FTIR spectrum of HC-1%Ce@ZnO after the fifth reuse cycle.

The reusability of HC-1%Ce@ZnO was evaluated over five successive MO degradation cycles (Figure 5b). After each cycle, the catalyst was recovered by centrifugation and calcined at 400 °C for 2 h before reuse. The degradation efficiency decreased from approximately 100% in the initial cycle to 80% after the first reuse and continued to decline to approximately 50% after the fifth reuse. The XRD pattern recorded after the fifth cycle (Figure 5c) retained the characteristic ZnO reflections observed for the fresh catalyst (Figure 2a). Likewise, the FTIR spectrum after the fifth cycle (Figure 5d) showed similar principal bands to those of the fresh catalyst (Figure 2b), with an additional band near 3420 cm^{-1} that may be associated with adsorbed water.

4. Conclusions

In this study, single crystals of Ce-doped ZnO nanoparticles with an average size below 10 nm were successfully biosynthesized using *Hedyotis capitellata* leaf extract in dual role of reacting and stabilizing agents. The integration of Ce into ZnO structure does not appear any new crystalline phase and the hexagonal wurtzite structures of pristine ZnO remains unchanged. In the comparison with the undoped ZnO, 1%Ce doped ZnO showed a superior photocatalytic degradation performance toward methyl orange. The photodegradation efficiency increased from

20% (HC-ZnO) to 92% (HC-1%Ce@ZnO) under a visible lamp illumination in 240 min. Thus, the biosynthesized Ce-doped ZnO has great potential as a prospective photocatalyst for wastewater decontamination applications.

References

[1] Adeel, M., Saeed, M., Khan, I., Muneer, M., & Akram, N. (2021). "Synthesis and characterization of Co-ZnO and evaluation of its photocatalytic activity for photodegradation of methyl orange." *ACS Omega* (6), 1426–1435. DOI: 10.1021/acsomega.0c05092

[2] Ahmad, R., Ali, A. M., Israf, D. A., Ismail, N. H., Shaari, K., & Lajis, N. H. (2005). "Antioxidant, radical-scavenging, anti-inflammatory, cytotoxic and antibacterial activities of methanolic extracts of some *Hedyotis* species." *Life Sciences* (76), 1953-1964. DOI: 10.1016/j.lfs.2004.08.039

[3] Al Farsi, B., Al Marzouqi, F., Al-Maashani, M., Souier, M. T., Myint, M. T. Z., & Al-Abri, M. Z. (2021). "Rapid microwave-assisted fabrication of Al-doped zinc oxide nanorods on a glass substrate for photocatalytic degradation of phenol under visible light irradiation." *Materials Science and Engineering: B* (264), 114977. DOI: 10.1016/j.mseb.2020.114977

[4] Bandeira, M., Giovanela, M., Roesch-Ely, M., Devine, D. M., & da Silva Crespo, J. (2020). "Green synthesis of zinc oxide nanoparticles: A review of the synthesis methodology and mechanism of formation." *Sustainable Chemistry and Pharmacy* (15), 100223. DOI: 10.1016/j.scp.2020.100223

[5] Davar, F., Majedi, A., & Mirzaei, A. (2015). "Green synthesis of ZnO nanoparticles and its application in the degradation of some dyes." *Journal of the American Ceramic Society* (98), 1739-1746. DOI: 10.1111/jace.13467

[6] Eljiedi, A. A. A., & Kamari, A. (2017). Removal of methyl orange and methylene blue dyes from aqueous solution using lala clam (*Orbicularia orbiculata*) shell. *Proceedings of the International Conference on Education, Mathematics and Science 2016 (ICEMS2016) in conjunction with 4th International Postgraduate Conference on Science and Mathematics 2016 (IPCSM2016), Perak, Malaysia, 2016* (AIP Conference Proceedings, tập 1847, mã bài 040003). Melville, New York: AIP Publishing. DOI: 10.1063/1.4983899.

[7] Golmohammadi, M., Honarmand, M., & Ghanbari, S. (2020). "A green approach to synthesis of ZnO nanoparticles using jujube fruit extract and their application in photocatalytic degradation of organic dyes." *Spectrochimica Acta Part A: Molecular and Biomolecular Spectroscopy* (229), 117961. DOI: 10.1016/j.saa.2019.117961

[8] Hasnidawani, J. N., Azlina, H. N., Norita, H., Bonnia, N. N., Ratim, S., & Ali, E. S. (2016). "Synthesis of ZnO nanostructures using sol-gel method." *Procedia Chemistry* (19), 211-216. DOI: 10.1016/j.proche.2016.03.095

[9] Hatamie, A., Khan, A., Golabi, M., Turner, A. P. F., Beni, V., Mak, W. C., Sadollahkhani, A., Alnoor, H., Zargar, B., Bano, S., Nur, O., & Willander, M. (2015). "Zinc oxide nanostructure-modified textile and its application to biosensing, photocatalysis, and as antibacterial material." *Langmuir* (31), 10913-10921. DOI: 10.1021/acs.langmuir.5b02341

[10] Kadam, A. N., Kim, T. G., Shin, D. S., Garadkar, K. M., & Park, J. (2017). "Morphological evolution of Cu doped ZnO for enhancement of photocatalytic activity." *Journal of Alloys and Compounds* (710), 102-113. DOI: 10.1016/j.jallcom.2017.03.150

[11] Kasinathan, K., Kennedy, J., Elayaperumal, M., Henini, M., & Malik, M. (2016). "Photodegradation of organic pollutants RhB dye using UV simulated sunlight on ceria based TiO_2 nanomaterials for antibacterial applications." *Scientific Reports* (6), 38064. DOI: 10.1038/srep38064

[12] Lang, J., Wang, J., Zhang, Q., Li, X., Han, Q., Wei, M., Sui, Y., Wang, D., & Yang, J. (2016). "Chemical precipitation synthesis and significant enhancement in photocatalytic activity of Ce-doped ZnO nanoparticles." *Ceramics International,* (42), 14175–14181. DOI: 10.1016/j.ceramint.2016.06.042

[13] Luu, T. V. H., Luu, M. D., Dao, N. N., Le, V. T., Nguyen, H. T., & Doan, V. D. (2020). "Immobilization of C/Ce-codoped ZnO nanoparticles on multi-walled carbon nanotubes for enhancing their photocatalytic activity." *Journal of Dispersion Science and Technology* (42) 1311-1322. DOI: 10.1080/01932691.2020.1740728

[14] Moezzi, A., McDonagh, A. M., & Cortie, M. B. (2012). "Zinc oxide particles: Synthesis, properties and applications." *Chemical Engineering Journal* (185-186), 1-22. DOI: 10.1016/j.cej.2012.01.076

[15] Nava, O. J., Soto-Robles, C. A., Gómez-Gutiérrez, C. M., Vilchis-Nestor, A. R., Castro-Beltrán, A., Olivas, A., & Luque, P. A. (2017). "Fruit peel extract mediated green synthesis of zinc oxide nanoparticles." *Journal of Molecular Structure* (1147), 1-6. DOI: 10.1016/j.molstruc.2017.06.078

[16] Phuong, N. M., Sung, T. V., Schmidt, J., Porzel, A., & Adam, G. (1998). "Capitelline: A new indole alkaloid from *Hedyotis capitellata*." *Natural Product Letters* (11), 93-100. DOI: 10.1080/10575639808041203

[17] Phuong, N. M., & Sung, T. V. (1999). "Two new β-carboline alkaloids from *Hedyotis capitellata* var.

mollis." *Planta Medica* (65), 761-762. DOI: 10.1055/s-2006-960861

[18] Rajendran, R., & Mani, A. (2020). "Photocatalytic, antibacterial and anticancer activity of silver-doped zinc oxide nanoparticles." *Journal of Saudi Chemical Society* (24), 1010-1024. DOI: 10.1016/j.jscs.2020.10.008

[19] Rodwihok, C., Wongratanaphisan, D., Van Tam, T., Choi, W. M., Hur, S. H., & Chung, J. S. (2020). "Cerium-oxide-nanoparticle-decorated zinc oxide with enhanced photocatalytic degradation of methyl orange." *Applied Sciences* (10), 1697. DOI: 10.3390/app10051697

[20] Saad, A. M., Abukhadra, M. R., Ahmed, S. A.-K., Elzanaty, A. M., Mady, A. H., Betiha, M. A., Shim, J.-J., & Rabie, A. M. (2020). "Photocatalytic degradation of malachite green dye using chitosan supported ZnO and Ce-ZnO nano-flowers under visible light." *Journal of Environmental Management* (258), 110043. DOI: 10.1016/j.jenvman.2019.110043

[21] Siddique, M., Fayaz, N., & Saeed, M. (2021). "Synthesis, characterization, photocatalytic activity and gas sensing properties of zinc doped manganese oxide nanoparticles." *Physica B: Condensed Matter* (602), 412504. DOI: 10.1016/j.physb.2020.412504

[22] Stan, M., Popa, A., Toloman, D., Dehelean, A., Lung, I., & Katona, G. (2015). "Enhanced photocatalytic degradation properties of zinc oxide nanoparticles synthesized by using plant extracts." *Materials Science in Semiconductor Processing* (39), 23-29. DOI: 10.1016/j.mssp.2015.04.038

[23] Subash, B., Krishnakumar, B., Velmurugan, R., Swaminathan, M., & Shanthi, M. (2012). "Synthesis of Ce co-doped Ag-ZnO photocatalyst with excellent performance for NBB dye degradation under natural sunlight illumination." *Catalysis Science & Technology* (2), 2319-2326. DOI:10.1039/C2CY20254A

[24] Ullah, R., & Dutta, J. (2008). "Photocatalytic degradation of organic dyes with manganese-doped ZnO nanoparticles." *Journal of Hazardous Materials* (156), 194-200. DOI: 10.1016/j.jhazmat.2007.12.033

[25] Wang, Z., Liu, Y., Huang, B., Dai, Y., Lou, Z., Wang, G., Zhang, X., & Qin, X. (2014). "Progress on extending the light absorption spectra of photocatalysts." *Physical Chemistry Chemical Physics* (16), 2758-2774. DOI: 10.1039/C3CP53817F

[26] Zhang, L., Qin, M., Yu, Y., Zhang, M., Zhao, X., Qian, J., & Wu, H. (2019). "Preparation of ternary Pt-NiO-ZnO hybrids and investigation of its photocatalytic performance toward methyl orange." *Journal of Materials Science: Materials in Electronics* (30), 5158-5169. DOI: 10.1007/s10854-019-00814-2

[27] Zhang, Y. G., Zhang, G. B., & Wang, Y. X. (2011). "First-principles study of the electronic structure and optical properties of Ce-doped ZnO." *Journal of Applied Physics* (109), 063510. DOI:10.1063/1.3561436